Thickness dependence of magnetization structures in thin Permalloy rectangles

Dedicated to Professor Dr. Helmut Kronmüller on the occasion of his 70th birthday

Riccardo Hertel*
Max-Planck–Institut für Mikrostrukturphysik, Weinberg 2, 06120 Halle, Germany

Zero-field magnetization states in Permalloy thin film elements of rectangular shape are calculated by means of finite element micromagnetic modeling. The energies of several possible magnetization patterns are determined for different sizes and thicknesses of the specimen. Based on these data, a phase diagram of the lowest-energy configuration is set up for rectangles of edge lengths between 250 nm and 1000 nm. It is shown that a thickness- and size-dependent transition from quasi-homogeneous single-domain states to demagnetized flux-closure patterns occurs in that range. The regime of sizes and thickness of the phase diagram in which the lowest-energy configuration of the thin film element is a single-domain state is particularly important, since in this case the sample is expected to show good stability with respect to thermal demagnetization, which is a required criterion to make it suitable for technological applications in magneto-electronic devices.

Keywords: Micromagnetic Modelling; Finite Element Method; Permalloy Thin-Film Elements; Single-Domain Limit

I. INTRODUCTION

In Magnetic Random Access Memory (MRAM) devices [1], soft magnetic thin film elements are used as unit cells of information. Ideally, each thin-film element of the device is homogeneously magnetized, with two possible directions of the magnetization, between which the particle can be switched. According to its magnetization direction, the information stored in an element is evaluated as either a logical "one" or a logical "zero". In real world, however, such soft magnetic platelets are generally not magnetically bistable systems. Instead, numerous different magnetic structures can be observed at zero field, depending on the particle's shape, size, material, thickness, its microstructure and its magnetic history. Most of these magnetization states are undesirable from a technological point of view, because once the magnetic structure splits up into a flux-closure magnetic domain pattern, the cell is no longer in a state which can be unambiguously assigned to a logical value. In Permalloy thin-film elements of rectangular shape, a large set of possible magnetic structures has been found both experimentally[2–4] and numerically [5, 6]. The agreement between calculated and observed structures is remarkably good. The domain structures can be categorized into remanent states with a high net magnetization, and flux closure patterns with vanishing average moment. The domain pattern of the latter ones are in perfect agreement with the construction scheme set up by Van Den Berg [7], an ingenuous geometrical algorithm to construct flux-closure patterns in ideally soft thin-film elements of arbitrary shape. The formation of these magnetic structures can usually be understood by considering Brown's pole avoidance principle[8] on one side and the tendency to avoid inhomogeneities of the magnetic structure on the other side. Remanent magnetic structures in soft magnetic elements are the outcome of a competition between stray field energy and exchange energy. When a hysteresis loop is performed with an in-plane field, it is generally not clear what exactly determines the resulting zero field configuration, especially if the sample drops in a demagnetized state. Which path, *e.g.* the magnetization takes from a saturated state to a demagnetized state with seven domains (diamond state[9]) as compared to the path from saturation to a Landau-type structure, either with or without cross-tie walls, and why the specimen chooses to drop into one state rather than the other are difficult questions which need to be examined with accurate time-resolved micromagnetic simulations. Obviously, the formation of end domains along those edges of the specimen which are aligned perpendicular to the external in-plane field is a decisive initial breaking of symmetry, which leads to different remanent states, known as C-state and S-state [10]. The C-state seems to be connected with the Landau-structure, while the S-state appears to be related with the diamond structure[11].

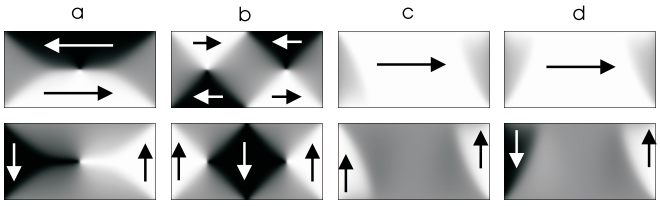

FIG. 1: Some basic magnetization structures in Permalloy rectangles. Demagnetized domain structures: (a) Landau, (b) Diamond; States with high remanence: (c) S-state, (d): C-state. The terms C-state and S-state are coined by the flux lines through the rectangle, having similar shapes as the respective letters.

In order to suppress closed-flux domain structures

*Electronic address: hertel@mpi-halle.mpg.de;
phone: +49-(0)345-5582-592
Fax: +49-(0)345-5511223

which may originate from such end domain patterns, elongated thin-films elements with tapered ends have been considered [2]. Indeed, these particles resulted to have one well-defined remanent state with almost uniform magnetization. Ambiguities connected with the possibility to obtain either C-state or S-state as remanent states and the resulting reduced stability with respect to the formation of flux-closure patterns were avoided. However other problems arose. While the remanent state was well-defined, the reversal mechanism was not, simply because the sources of possible instabilities had been successfully suppressed. As a consequence of this, the location at which the reversal nucleates is almost unpredictable in such particles. Even computations lead to different results, some claiming the reversal starts in the middle of the sample[12], others stating that a vortex penetrates the sample from the side of the specimen[13], both of which are likely to be possible. Nowadays, the formation of end domains is seen as a helpful feature, because they allow the magnetization to reverse continuously by means of edge soliton propagation. In this case, the magnetization of the particle switches by the nucleation of head-on domain walls moving along the edges, which is preceded by an expansion of the end domains. However, it is important to have control of the end domains, in order to allow for a reproducible switching process. It has been shown earlier, that the S-state switches in a continuous fashion [5, 14], with two edge solitons which propagate along the edge without intersecting. Therefore, a switching process between two S-states is generally not problematic, whereas C-states are difficult to switch[6]. Recently, Arrott [29] has proposed the use of thin-film elements with specially rounded corners – similar to the shape of a bean – in order to favor the C-state as a remanent state, to suppress accidental switching. The reversal of this particle should occur by means of an additional bias field, which converts the structure into the S-type, thus allowing to switch easily.

One of the major challenges in the technical application of magnetic thin film elements for MRAM devices is the required reliability and reproducibility of the switching process. Over more than 10^{13} cycles of magnetization reversal, the particle is required to remain magnetized in a well-defined high-remanence state. Therefore, the number of possible demagnetized states needs to be kept as small as possible, in order to reduce the probability of an accidental demagnetization, driven, *e.g.*, by thermal effects. Contrary to the aforementioned approaches, which focus on different *shapes* of thin film elements, this paper reports on the influence of the *thickness* of a thin film element on the total energy of domain structures. If a thin film element is a single-domain particle in the sense that a flux-closure magnetization pattern has a higher energy than a structure with high remanence, it is unlikely to drop accidentally in a demagnetized states, and it is important to know whether this property can be obtained by simply changing the particle's thickness.

Several magnetic structures in Permalloy thin film elements of rectangular shape (aspect ratio 2:1) are investigated, and their energy is compared as a function of the specimen's thickness. The investigations are carried out using a micromagnetic finite element algorithm.

II. MICROMAGNETIC BACKGROUND

The most significant energy terms to be considered for the calculation of remanent magnetic structures in the framework of micromagnetism are exchange, anisotropy and stray field energy:

$$E_{\rm tot} = \int\limits_{(V)} \sum_{i=x,y,z} A(\boldsymbol{\nabla} \boldsymbol{m}_i)^2 + K\left[1-(\boldsymbol{m}\cdot\boldsymbol{k})^2\right] - \frac{\mu_0}{2}\boldsymbol{M}\cdot\boldsymbol{H}_{\rm s}{\rm d}V \tag{1}$$

In the case of Permalloy, surface anisotropy is negligible, and since we are interested in zero field configurations, the Zeeman term is omitted. To mimic the properties of Permalloy, an exchange constant A=1.3·10^{-11} J/m, a uniaxial anisotropy constant $K = 500\,{\rm J/m^3}$, and a saturation magnetization $M_{\rm s} = |\boldsymbol{M}| = 7.96 \cdot 10^5 {\rm A/m}$ corresponding to a saturation polarization $J_{\rm s} = \mu_0 M_{\rm s}$ of 1.00 T, are assumed. In Eq. (1), $\boldsymbol{m} = \boldsymbol{M}/M_{\rm s}$ denotes the reduced magnetization and $\boldsymbol{k}$ is a unit vector parallel to the easy axis, which is is along the long edge of the rectangle. The stray field $\boldsymbol{H}_{\rm s}$ is the magnetic field arising from the magnetic moments of the sample. A detailed description of the calculation of this contribution is given in the next section.

Equilibrium configurations of the magnetization can be obtained by minimizing the total energy $E_{\rm tot}$ with respect to the directional field of the magnetization, *i.e.*, by solving the variational problem $\delta E_{\rm tot} = 0$, where $E_{\rm tot}$ is uniquely determined by the magnetic structure $\boldsymbol{M}(\boldsymbol{r})$. Stable magnetic structures correspond to local energy minima of the magnetic configurational space. Generally, analytic solutions of this variational problem are only available for samples of special, simple geometry and by making use of simplifying assumptions concerning the magnetic structure and the demagnetizing field $\boldsymbol{H}_{\rm s}$. However, by means of numerical calculations, magnetization structures can be calculated from first principles in the framework of micromagnetism. Such simulations generally represent a difficult task, and they are usually restricted to particles in the sub-micrometer range. This is mostly so because of the high system requirements (memory, processing time) involved with the numerical calculation of the long-range interaction given by the stray field, which grow rapidly with increasing number of discretization cells. The restrictions in size are also due to the disparate length scales involved in micromagnetic problems. Widely extended regions of homogeneous regions (the magnetic domains) are connected by narrow regions of strongly inhomogeneous magnetization (the domain walls). The important length scales describing these features, first introduced by Kronmüller[15], are the so-called exchange lengths. They

describe the typical extension of magnetic microstructures. In soft magnetic materials the exchange length of the stray field $l_s = \sqrt{2A/\mu_0 M_s^2}$ is decisive, whereas in hard magnetic materials the exchange length due to the anisotropy $l_K = \sqrt{A/K}$ needs to be considered. These exchange lengths are connected with the extension of Néel walls and Bloch walls[16], respectively. A powerful method to account for the different length scales in micromagnetic simulations has been presented by Hertel and Kronmüller, who developed two different adaptive mesh refinement schemes for three-dimensional micromagnetic calculations, thus allowing to accurately simulate the magnetic structure in samples of unprecedented size [17].

Increased experimental ability of nano-patterning of thin film elements, on one side, and the steadily growing computational power combined with improving numerical techniques, on the other side, have shifted the typical size of samples which can be calculated reliably in the range of particles as they are experimentally produced and technologically relevant. In fact, it is nowadays possible to perform micromagnetic simulations on elements of larger size than those planned to be used in future magneto-electronic devices. A potential memory element as it could be used in an MRAM should have a lateral extension in the sub-micron range.

III. FINITE ELEMENT MICROMAGNETIC MODELING

To calculate numerically the field of the magnetization, a discretized form of it is first required. For this purpose, the sample is subdivided into simplex elements, *i.e.* tetrahedral elements in the three-dimensional case. The orientation and the shape of these elements is generally irregular, which allows to approximate the shape of samples of virtually arbitrary shape. This is in strong contrast to the commonly used finite-difference schemes, which require a regular discretization mesh of cube-shaped cells of equal size. In the latter case, inclined or curved surfaces need to be approximated with a "staircase" approximation. Only in two-dimensional simulations, and with considerable effort, it has recently become possible to obtain some remedy of the errors arising from this approximation [18]. The geometrical flexibility of the finite element method has been exploited to perform simulations of materials with complicated, realistic grain structures [19, 20] and to adaptively refine specific parts of the computational region, wherever a higher discretization density is required [21].

Numerically, the minimization of the total energy (1) is performed with a conjugate gradient method [22]. The constraint of constant magnitude of the magnetization $|\boldsymbol{M}| = \text{const.}$ needs to be observed during the minimization process, which can be achieved easily by representing the magnetization vector with spherical coordinates φ, ϑ.

It is noteworthy that within each element a linear interpolation of the magnetization is used. The interpolation is performed using so-called shape functions, which allow to determine a value of a discretized function inside each finite element by means of interpolation of the values on the discretization points, which are just the corner points of the elements in this case. Compared with the zero-order approximations used in algorithms based on finite differences and the evaluation of the stray field by means of Fast Fourier Transformation (FFT) [23], where the magnetization is assumed to be piecewise *homogeneous*, this first-order interpolation scheme with a piecewise *linear* approximation is more precise concerning the calculation of the stray field term. By using a linear interpolation scheme, inhomogeneous magnetization pattern do not perform sudden, unphysical discontinuities at the boundaries of the discretization cells, contrary to zero-order schemes, where this effect can lead to fictitious uncompensated charges, which may be sources of errors in the calculation of the stray field term. The drawback of the finite element method is that the implementation is quite complicated and the memory requirements are higher than those needed in finite-difference schemes.

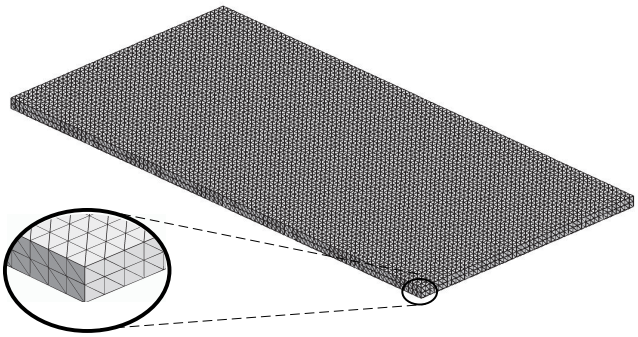

FIG. 2: Finite element mesh used for the simulations. The edges of the elements are represented as a wireframe. The mesh consists of 15 000 nodes placed on a regular grid, which are the corner points of 58 212 tetrahedral elements. Inside the elements the magnetization is interpolated linearly.

Having the discretization scheme with the corresponding interpolation functions, the evaluation of the micromagnetic energy terms is generally straightforward. The only term which requires a closer look is the long-range term resulting from the stray field. To calculate the stray field, a scalar potential U is introduced, from which $\boldsymbol{H}_s$ is derived as a gradient field $\boldsymbol{H}_s = -\boldsymbol{\nabla} U$. The potential U satisfies Poisson's equation

$$\Delta U = 4\pi \nabla \boldsymbol{M} \tag{2}$$

with the boundary conditions

$$U_i|_{\partial V} = U_o|_{\partial V} \quad , \tag{3}$$

$$\left.\frac{\partial U_{\mathrm{i}}}{\partial \hat{\boldsymbol{n}}}\right|_{\partial V} - \left.\frac{\partial U_{\mathrm{o}}}{\partial \hat{\boldsymbol{n}}}\right|_{\partial V} = -4\pi \hat{\boldsymbol{n}} \cdot \boldsymbol{M} \qquad (4)$$

and

$$\lim_{x \to \infty} U = 0 \qquad (5)$$

where U_{i} and U_{o} are the inward and the outward limit of the potential at the surface ∂V and $\hat{\boldsymbol{n}}$ is the normal vector directed out of the sample.

To solve Poisson's equation with proper consideration of the boundary conditions, the boundary element method (BEM) is combined with the finite element method (FEM). Highly accurate calculations can be obtained by means of this hybrid FEM/BEM scheme, which was first applied to micromagnetic problems by Fredkin and Koehler[24]. The ansatz used to solve Eq. (2) is to split the potential U into two parts $U = U_1 + U_2$. One part of the potential, U_1, is zero outside the magnetic particle and satisfies Poisson's equation inside the sample. The Neumann boundary conditions (4) are natural conditions in the solution of U_1. The other part, U_2, is a solution of Laplace's equation. The Dirichlet boundary conditions for U_2, which uniquely determine the solution, are obtained from the values of U_1 at the particle's surface ∂V by means of a boundary integral[24]

$$\begin{aligned} U_2(\boldsymbol{x}) &= \frac{1}{4\pi} \int_{\partial V} U_1(\boldsymbol{x'}) \frac{\partial}{\partial \hat{\boldsymbol{n}}(\boldsymbol{x'})} \frac{1}{|\boldsymbol{x} - \boldsymbol{x'}|} \, \mathrm{d}S' \\ &\quad + \left(\frac{\Omega(\boldsymbol{x})}{4\pi} - 1 \right) U_1(\boldsymbol{x}) \quad , \end{aligned} \qquad (6)$$

where the integral is extended over the surface ∂V and $\Omega(\boldsymbol{x})$ is the solid angle subtended at the surface point $\boldsymbol{x}$. Numerically, the elliptical differential equations are solved with the Galerkin method, by means of which the discretized problem is transformed into a (large) set of linear equations that can be solved with the biconjugate gradient method. After the stray field of a magnetic structure is calculated, the minimum energy arrangement of the magnetization is determined. The process of calculating the magnetic structure and its stray field is iteratively repeated until a self-consistent solution is obtained.

IV. MAGNETIC STRUCTURES IN PERMALLOY RECTANGLES

Soft magnetic thin film elements are magnetized in-plane because of the predominant influence of the stray field energy ("shape anisotropy"). The tendency to arrange the in-plane magnetization in a way to form magnetic domains is due to the finite lateral extension. Surface charges at the boundary of the sample can be avoided by aligning the magnetization parallel to the edges, as is the case in flux-closure patterns. Obviously, the driving force to form magnetic domains diminishes

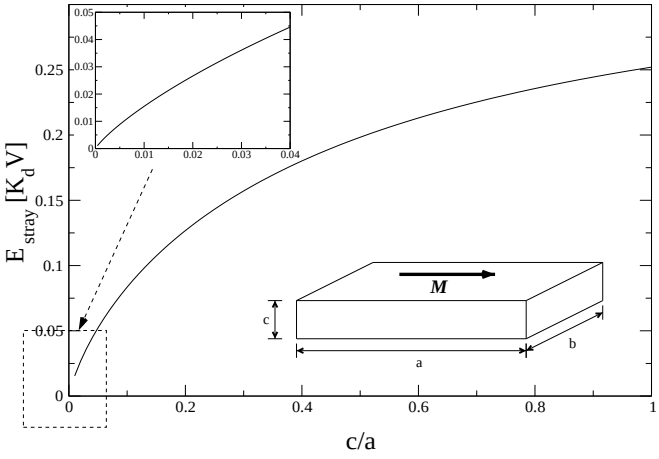

FIG. 3: Average stray field energy density of rectangular particles with aspect ratio $a : b$=2:1, homogeneously magnetized along the long edge (a) as a function of the relative thickness c/a. The values are calculated using the equations due to Aharoni. The energy density E_{stray}/V is given in units of the stray field constant $K_d = \mu_0 M_{\mathrm{s}}^2/2$.

with the particle's thickness, because the amount of surface charges arising from a homogeneous in-plane magnetization depends on the area of the surface to which the magnetization is perpendicularly oriented. Analytic expressions on the stray field energy of homogeneously magnetized prisms have been provided by Aharoni[25]. Quantitatively, the thickness dependence of the average energy density of a homogeneously magnetized slab is shown in the diagram of Fig. 3. As can be seen in the inset, especially in the thin-film regime the increase in energy with thickness is particularly steep, and almost linear.

The energies resulting from the analytical calculations represent upper bounds for real rectangles with single-domain in-plane magnetization. If a rectangular thin film element is magnetized along the long edge, surface charges (and stray field energy) are reduced by the formation of end domains, which lead to the aforementioned C- and S-states. Still, these structures have considerable stray field energy, which can be reduced by means of flux-closure arrangements, however at the expense of exchange energy due to the domain walls. Contrary to the stray field energy density of a homogeneously magnetized thin film element, the energy density of an idealized multi-domain structure with flux closure does not depend on the thickness, provided that the magnetization does not vary along the thickness. This thickness dependence of the stray field energy eventually leads to a transition from a single-domain state to a multi-domain state.

To give an overview of the dependence on size and thickness of magnetic structures in thin Permalloy rectangles, the energy of various magnetization states is calculated in different platelets. The particles have edge lengths ranging between 250 nm×125 nm and 1000 nm×500 nm, which is in the order of the technologi-

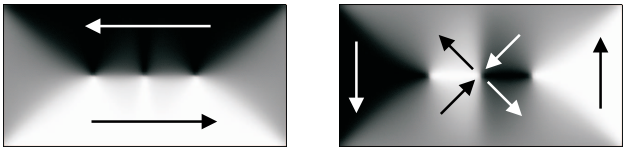

FIG. 4: The two major domains of a Landau-type structure can be separated by a cross-tie wall. This wall type is often found in soft magnetic thin films of intermediate thickness (10-50 nm) .

cally relevant size. The thickness of the rectangles is varied between 2.5 nm and 32.5 nm. Since the aspect ratio of the rectangles $a : b$ is equal to 2:1 in all cases, the long edge a and the thickness c are sufficient to specify the sample's dimensions. In addition to the magnetic patterns shown in Fig. 1 a cross-tie wall structure as shown in Fig. 4 is taken into consideration.

The resulting energies are shown in Fig. 5, as a function of the thickness for four rectangles of different size. Generally, the average energy density of the high-remanence C- and S-states increases with the thickness, in accordance with the behavior expected from analytic calculations, cf. Fig. 3. Although not recognizable from Fig. 5, in all cases the C-state has a lower energy than the S-state. The reason for this is probably that the surface charges of opposite sign, which attract each other, are closer together in the C-state than in the S-state.

In the range of size and thickness considered here, the cross-tie structure is never a lowest-energy arrangement. For very thin and small platelets, the cross-tie structure is numerically unstable and converts into the Landau-structure. With increasing size, obviously, the tendency to form flux-closure domain patterns increases with the size (both thickness and edge length), so that the average energy density of Landau, Diamond and cross-tie structures decreases with the edge length.

Although the energy of the different patterns can differ significantly with the size, the magnetic structures are largely independent on size and thickness. As shown in Fig. 6, the patterns are mostly invariant with respect to scaling. In the C-state, however, the domain walls become somewhat sharper and the subdivision into domains clearer as the particle's size increases.

It is a difficult task to identify a structure as a magnetic ground state of a particle, because it can not be ruled out strictly that some structure which has not been taken into consideration has a lower total energy than the lowest-energy arrangement of the calculated structures. This situation occurred in Standard Problem No. 3 [26, 27] in which a small ferromagnetic cube was considered, and the transition between two magnetization states (Flower State and Vortex State) was calculated. This was supposed to be a size-dependent transition between two magnetic ground states. Later, Hertel and Kronmüller have shown that a third state, which was named Twisted Flower State, has a lower energy at the relevant edge lengths [28]. In small thin film ele-

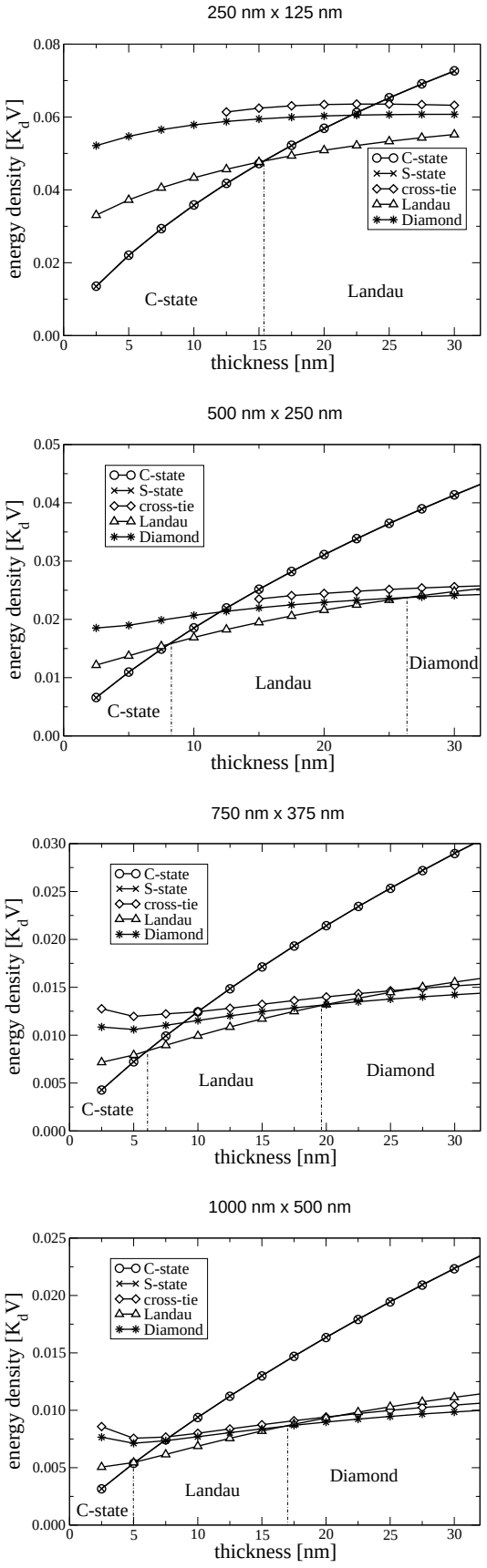

FIG. 5: Average energy densities of different magnetization states in rectangular platelets as a function of the thickness. The lowest-energy arrangement is marked in the corresponding regions.

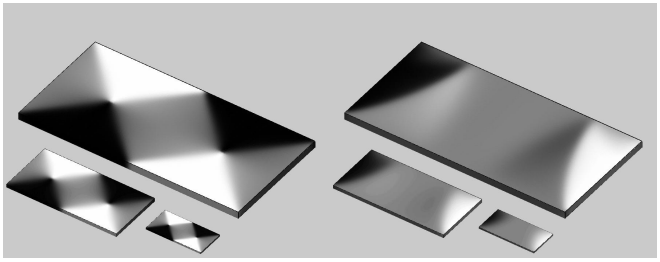

FIG. 6: Perspective view on platelets of different size, however with same aspect ratio. On the left side, the platelets are in the diamond state, on the right the magnetization is in the C-state. The major edge lengths are 1000 nm, 500 nm, and 250 nm, the thicknesses are 30, 15, and 7.5 nm, respectively. Note that the particles are only graphically placed next to each other. The micromagnetic calculations are performed for isolated, non-interacting platelets.

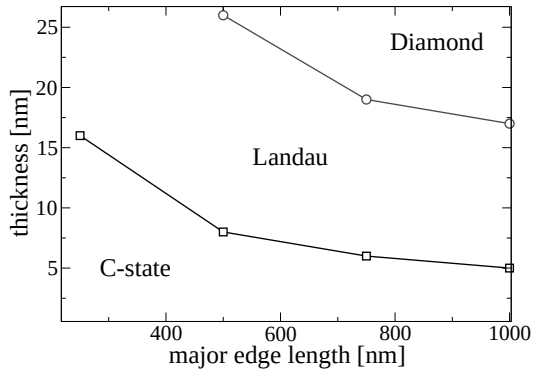

FIG. 7: Phase diagram of the lowest-energy arrangement in Permalloy rectangles of aspect ratio 2:1.

ments, where the magnetization structure is essentially two-dimensional, the manifoldness of possible magnetic structures is probably smaller, so that the set of magnetization states presently considered is likely to be sufficient. The symmetric in-plane Flower state has not been considered (in the nomenclature of C- and S-state, this one could be referred to as "X-state"). Though this structure might occur in very small platelets, it is unstable in larger rectangles and there it has a higher energy than S- or C-state due to the inefficient reduction of surface charges. Also not considered is a double cross-tie wall structure, which could become stable in thick and large platelets but is unstable at smaller sizes. Moreover, not even the single cross-tie pattern is an energetically convenient arrangement in the range of size considered here, and a two-fold cross-tie structure requires larger lateral extensions than a single one to sustain the two cross-tie walls.

Based on the data as presented in Fig. 5 a phase diagram according to Fig. 7 can be set up. According to this, a single-domain regime, where the high-remanence structures C-state and S-state have the lowest energy can be clearly identified depending on size and thickness. For a rectangular platelet with dimensions corresponding to this regime, flux-closure patterns have a higher energy than the quasi-homogeneous states. Such particles can therefore be expected to be more unlikely to drop accidentally into a technologically undesirable flux-closure domain state.

[1] L. Zhu, Y. Zheng, and G. Prinz, J. Appl. Phys. **87**, 6668 (2000).

[2] K. J. Kirk, J. N. Chapman, and C. D. W. Wilkinson, J. Appl. Phys. **85**, 5237 (1999).

[3] R. D. Gomez, T. Luu, A. Pak, I. Mayergoyz, K. Kirk, and J. Chapman, J. Appl. Phys. **85**, 4598 (1999).

[4] A. Hubert and R. Schäfer, *Magnetic Domains - The Analysis of Magnetic Microstructures* (Berlin, New York, Heidelberg: Springer, 1998).

[5] H. Kronmüller and R. Hertel, J. Magn. Magn. Mater. **215-216**, 11 (2000).

[6] W. Rave and A. Hubert, IEEE Trans. Magn. **36**, 3886 (2000).

[7] H. A. M. Van Den Berg and A. H. J. Van Den Brandt, J. Appl. Phys. **62**, 1952 (1987).

[8] W. F. Brown, Jr., *Magnetostatic Principles in Ferromagnetism* (North-Holland publishing company, Amsterdam, 1962).

[9] R. Hertel and H. Kronmüller, J. Appl. Phys. **85**, 6190 (1999).

[10] Y. Zheng and J. Zhu, J. Appl. Phys. **81**, 4336 (1997).

[11] R. Hertel and H. Kronmüller, Physica B **275**, 1 (2000).

[12] J. Gadbois, J. G. Zhu, W. Vavra, and A. Hurst, IEEE Trans. Magn. **34**, 1066 (1998).

[13] T. Schrefl, J. Fidler, K. J. Kirk, and J. N. Chapman, J. Magn. Magn. Mater. **175**, 193 (1997).

[14] R. H. Koch, D. J. G., W. Abraham, P. Trouilloud, R. Altman, Y. Lu, W. J. Gallagher, S. R.E., and S. Parkin, Phys. Rev. Lett. **81**, 4512 (1998).

[15] H. Kronmüller, Zeitschrift für Physik **168**, 478 (1962).

[16] H. Kronmüller and M. Lambeck, in *Lehrbuch der Experimentalphysik*, edited by W. de Gruyter (Bergmann, Schaefer, Berlin, New York, 1992), vol. 6, pp. 715–791.

[17] R. Hertel and H. Kronmüller, Phys. Rev. B **60**, 7366 (1999).

[18] Z. Gimbutas, C. Garcia-Cervera, and E. Weinan, submitted to Journal of. Comp. Phys. (2001).

[19] T. Schrefl, H. Kronmüller, and J. Fidler, J. Magn. Magn. Mater. **127**, L273 (1993).

[20] R. Fischer and H. Kronmüller, Phys.Rev.B **54**, 7284 (1996).

[21] R. Hertel and H. Kronmüller, IEEE Trans. Magn. **34**, 3922 (1998).

[22] W. H. Press, B. P. Flannery, S. A. Teukolsky, and W. T. Vetterling, *Numerical Recipies: The art of scientific computing* (Cambrige Univeristy Press, Cambrige, New York,

1986).
[23] D. Berkov, K. Ramstöck, and A. Hubert, Phys. Stat. Sol. (a) **137**, 207 (1993).
[24] D. R. Fredkin and T. R. Koehler, IEEE Trans. Magn. **26**, 415 (1990).
[25] A. Aharoni, J. Appl. Phys. **83**, 3432 (1998).
[26] W. Rave, K. Fabian, and A. Hubert, J. Magn. Magn. Mater. **190**, 332 (1998).
[27] R. D. McMichael, *Standard problem number 3, Problem specification and reported solutions* (Micromagnetic Modeling Activity Group, `http://www.ctcms.nist.gov/~rdm/mumag.html`, 1998).
[28] R. Hertel and H. Kronmüller, J. Magn. Magn. Mater. **238**, 185 (2002).
[29] A.S. Arrott, private communication (2001)